

# INTERNATIONAL SOCIETY FOR SOIL MECHANICS AND GEOTECHNICAL ENGINEERING



*This paper was downloaded from the Online Library of the International Society for Soil Mechanics and Geotechnical Engineering (ISSMGE). The library is available here:*

<https://www.issmge.org/publications/online-library>

*This is an open-access database that archives thousands of papers published under the Auspices of the ISSMGE and maintained by the Innovation and Development Committee of ISSMGE.*

## Water Distribution System Response to the 22 February 2011 Christchurch Earthquake

D. Bouziou<sup>1</sup>, T.D. O'Rourke<sup>2</sup>

### ABSTRACT

The response of the Christchurch water distribution system to transient and permanent ground deformations during the 22 February 2011 earthquake is evaluated through geospatial analysis, using the most recent water pipeline repair records and high resolution light detection and ranging (LiDAR) data. Repair rates, expressed as repairs/km, for different types of pipeline are correlated with 1) peak ground velocity outside liquefaction areas, and 2) differential ground surface lateral and vertical movements in liquefaction areas. Polyvinyl chloride pipelines are shown to be markedly more resilient to earthquake effects than other types of segmental pipelines in the Christchurch system. The level of LiDAR resolution is shown to have substantial influence on the relationship between pipeline damage and lateral ground strain. Repair regressions are presented that quantify the performance of different pipelines under different levels of ground deformation.

### Introduction

The response of the Christchurch water distribution system during the 22 February 2011 earthquake to transient and permanent ground deformations (TGD and PGD, respectively) is investigated in geospatial analysis, using a database that includes the most recent water repair records, strong motion recordings, high resolution Light Detection and Ranging (LiDAR) survey data, and Geographical Information System (GIS) maps of the Christchurch water distribution system and areas of observed liquefaction. Repair rates (RR), expressed as repairs/km, for different pipe types are correlated with 1) peak ground velocity outside liquefaction areas, and 2) differential ground surface lateral and vertical movements in liquefaction areas. Regressions are compared between RR and lateral ground strains derived from LiDAR ground movements at 4-m and 56-m spacing. Relationships among RR, differential vertical ground movement, and lateral ground strains are developed from the repair records and LiDAR data.

### GIS Database

Figure 1 shows a map of the Christchurch water distribution system. Geospatial data for the 22 Feb. 2011 earthquake include approximately 1700 km of water mains, ranging from 75 to 600 mm in diameter, with internal pressure of about 100 kPa. Airborne Light Detection and Ranging (LiDAR) data were obtained for vertical and lateral ground movements at 5-m as well as 4-m and 56-m spacing, respectively. The fundamental vertical accuracy of the LiDAR is between  $\pm 7$  cm and  $\pm 15$  cm, whereas the horizontal accuracy, compared to land survey measurements, is 40 to 55 cm (CERA, 2012). A GIS shapefile with the areas of observed liquefaction effects was

---

<sup>1</sup>Civil Engineer, Iperidou 9, Edafos Engineering Consultants S.A., Athens, Greece, 10558, [db552@cornell.edu](mailto:db552@cornell.edu)

<sup>2</sup>Thomas R. Briggs Professor, 273 Hollister Hall, Cornell University, Ithaca, NY 14853, [tdo1@cornell.edu](mailto:tdo1@cornell.edu)

obtained through the Canterbury Geotechnical Database (CERA, 2012) and modified as described by O'Rourke, et al (2014). The geometric mean peak ground velocity (GMPGV) was calculated for each of 40 stations as the mean of the natural logs of the two maximum horizontal peak ground velocities available from GNS Science (2013).

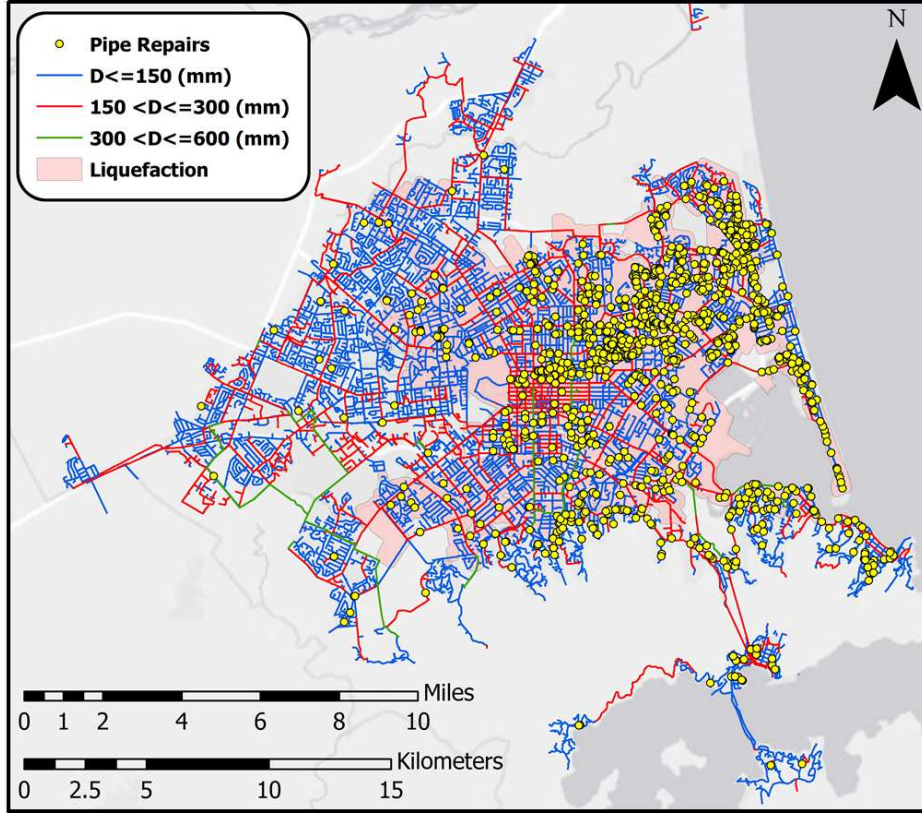


Figure 1. Map of Christchurch water distribution system during the 22 Feb. 2011 earthquake.

Table 1 summarizes lengths, repairs, and RRs for asbestos cement (AC), cast iron (CI), polyvinyl chloride (PVC), and modified polyvinyl chloride (MPVC) pipelines, including locations inside and outside areas of liquefaction effects. The category of “other” includes pipe types present in relatively small quantities. Pipeline damage was mostly concentrated inside the areas of observed liquefaction effects. The PVC and MPVC pipelines performed significantly better than their AC and CI counterparts.

### Screening Criteria

The screening criteria developed by O'Rourke et al. (2014) were used in all RR correlations to ensure that pipeline intervals of sufficient length were chosen for robust statistics. The minimum sampling length,  $x$ , needed for a confidence interval,  $\beta_c$ , that the actual number of repairs falls within  $\pm \alpha$  of the mean value  $(RR)x$  is given as follows

$$x \geq \frac{[\phi^{-1}(\beta_c)]^2}{\alpha^2(RR)} \quad (1)$$

in which  $x$  is sampling length,  $\alpha$  is a fraction of actual repairs,  $RR$  is repair rate, and  $\phi^{-1}(\beta_c)$  is the standard normal deviate for a confidence level  $\beta_c$ , corresponding to the sampled number of

repairs falling within  $\pm \alpha$  of the mean number of repairs. For this study  $\alpha$  was chosen as 0.5, and a relatively high confidence interval  $\geq 90\%$  was applied in most cases. The confidence interval was reduced in some cases to produce RR data over a broader range of ground deformation.

Table 1. Statistics of water main repairs and repair rates for the 22 February 2011 earthquake.

Pipe Material	Pipe Length (km)	Repairs	Overall Average RR	% Repairs in LIQ <sup>1</sup> areas	% Pipeline in LIQ <sup>1</sup> areas	% Damaged Pipeline in LIQ <sup>1</sup> areas	% Damaged Pipeline in Non LIQ <sup>1</sup> areas	Average RR in LIQ <sup>1</sup> areas	Average RR in Non LIQ <sup>1</sup> areas
AC	867.2	1024	1.18	85%	47%	16%	3%	2.15	0.33
CI	194.4	255	1.31	89%	67%	14%	3%	1.73	0.44
PVC	213.6	68	0.32	93%	52%	5%	1%	0.56	0.05
MPVC	149.7	13	0.09	100%	33%	2%	0%	0.27	0.00
Other	305.4	142	0.47	83%	83%	4%	4%	0.46	0.47
Total	1730.3	1502	0.87	86%	55%	11%	2%	1.36	0.27

<sup>1</sup> LIQ: Areas of liquefaction effects.

### RR Correlations with GMPGV

The spatial distribution of GMPGV was interpolated from the recorded ground motions using ordinary kriging with a spherical variogram that accounts for anisotropy. Figures 2a and 2b show the areas of liquefaction effects, water distribution pipelines, repairs outside liquefied areas, and 10 cm/sec contours of GMPGV for the 22 Feb. 2011 earthquake, pertaining to AC and CI distribution mains, respectively.

The RRs for AC pipelines and various GMPGVs for the 22 Feb. 2011 earthquake are shown in Figure 3a combined with similar data reported by Jeon (2002) for AC pipelines. Two data points for the 22 Feb. 2011 earthquake are combined with historical data reported by Jeon and O'Rourke (2005) to develop the linear regressions for CI pipelines in Figure 3b. The linear regressions for AC and CI pipelines using data from the 22 Feb. 2011 and previous earthquakes are comparable and indicate their similar response to PGV.

### RR Correlations with Differential Vertical Ground Movement

The set of vertical ground surface movements at 5-m spacing before and after the 22 Feb. 2011 earthquake was used to develop RR correlations with differential vertical ground movement for the 22 Feb. 2011 earthquake. The data were corrected for tectonic movements using dislocation models provided by GNS Science (2013). Ground angular distortion,  $\beta$ , is defined as the gradient of settlement between two adjacent measurement points

$$\beta = \frac{\delta z_1 - \delta z_2}{l_{12}} \quad \beta = \frac{\delta z_1 - \delta z_2}{l_{12}} \quad (2)$$

where  $\delta z_1$  and  $\delta z_2$  are the vertical movements of points 1 and 2, respectively, and  $l_{12}$  is the distance between the two points in the horizontal plane.

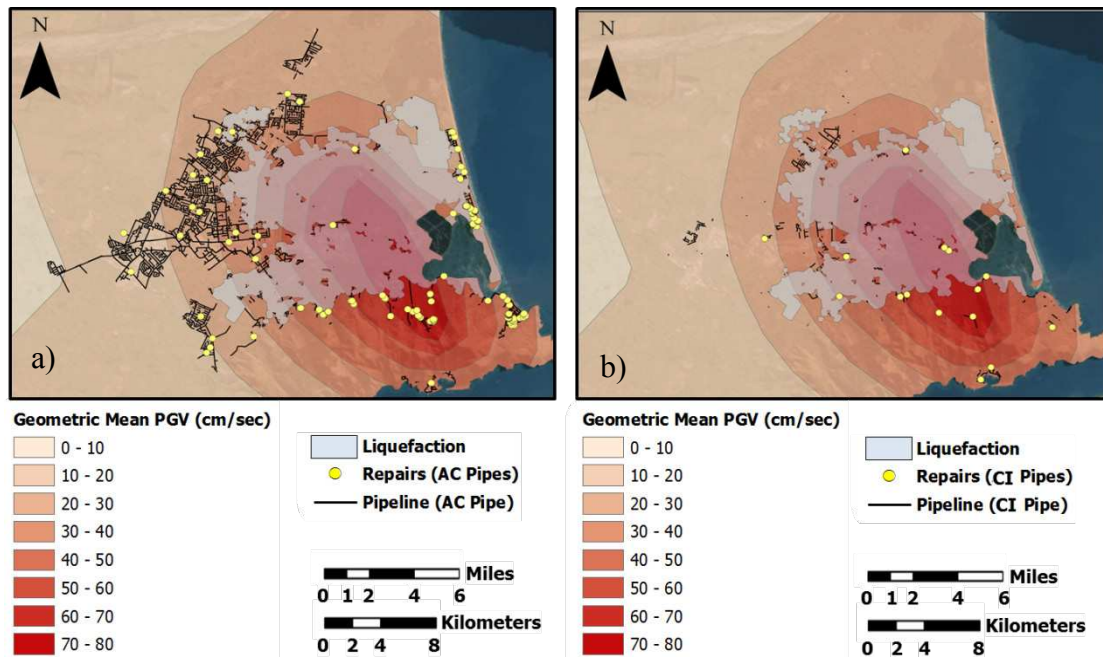


Figure 2. a) 22 Feb. 2011 earthquake map of GMPGV and liquefaction with AC pipelines and repairs, and b) 22 Feb. 2011 earthquake CI pipeline layout, repairs, and map of GMPGV.

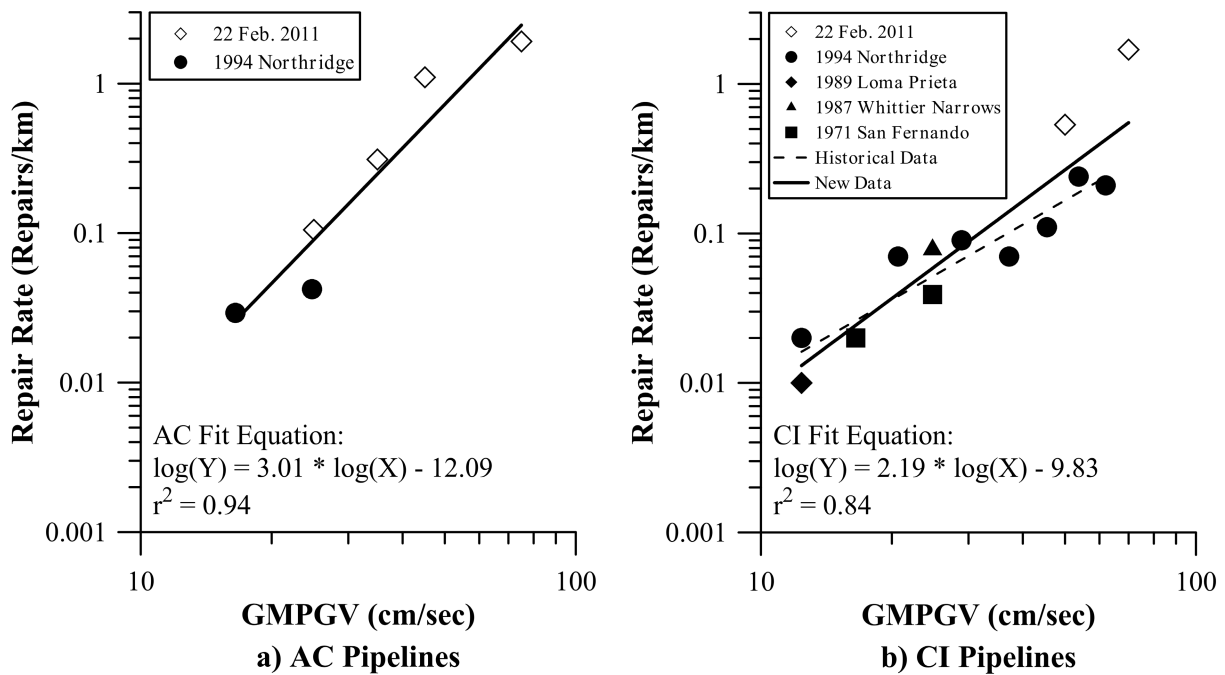


Figure 3. Repair rate vs. GMPGV for a) AC pipelines and b) CI pipelines.

The analytical process for RR correlations with  $\beta$  described by Bouziou (2015) was used to develop the regression results for  $\beta$  presented in Figure 4a. Confidence levels of 95%, 90%, and 75% were used in the screening criteria for correlations of RR with  $\beta$  for AC, CI, and PVC

pipelines, respectively, to allow for more RR values to be provided in the linear regression for each pipe type over a suitable range of  $\beta$ . Figure 4b compares the results of the current investigation, using the most recent repair records, with the results of previous work (O'Rourke et al., 2014). The regressions for each pipe type in the current and previous studies compare favorably with each other.

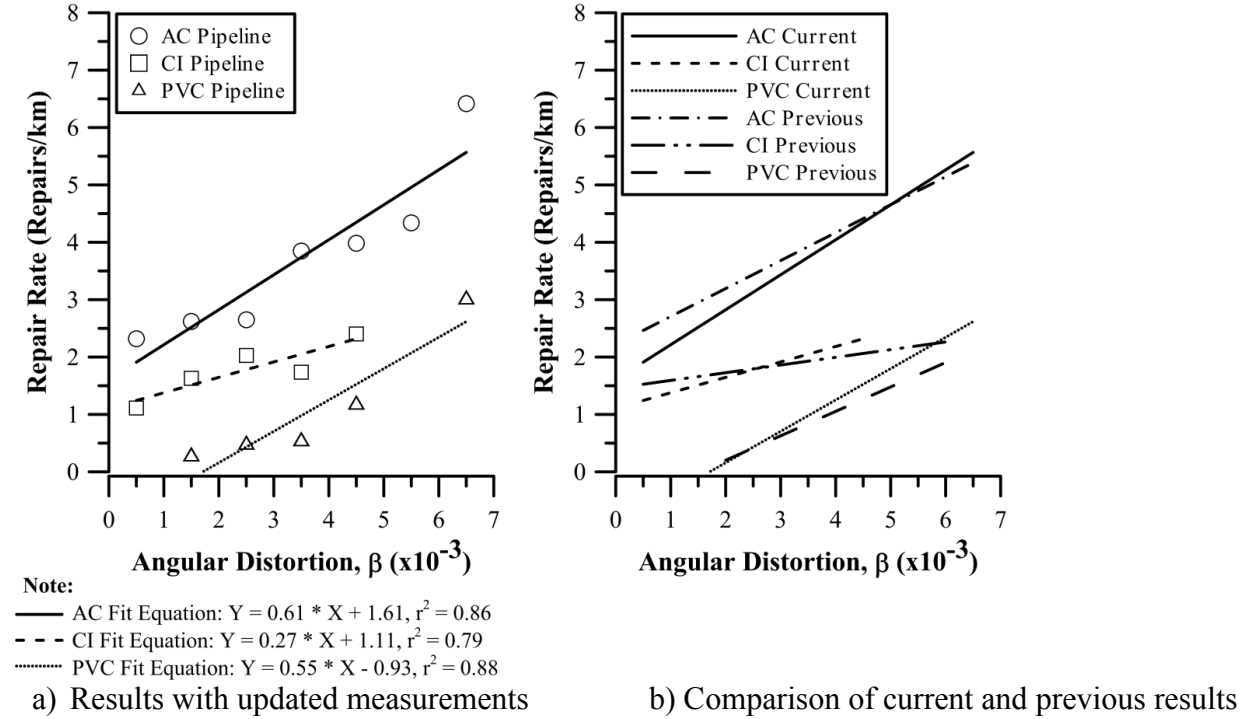


Figure 4. Repair rate vs. angular distortion for AC, CI, and PVC pipelines.

### RR Correlations with Lateral Ground Strain

LiDAR lateral ground movements at 4-m and 56-m spacing were used to calculate lateral ground strains and develop RR correlations. Similar to LiDAR vertical movements, the LiDAR horizontal movements were also corrected for tectonic movements. The process described by Bouziou (2015) for developing RR vs lateral ground strain regressions was followed, and the lateral ground strains were calculated using the methodology presented by O'Rourke et al. (2014). The absolute maximum value of lateral ground strain,  $\epsilon_{HP}$ , in each elemental area of ground was used as a metric for RR correlations with lateral ground strain given by

$$\epsilon_{1,2} = \frac{\epsilon_x + \epsilon_y}{2} \pm \sqrt{\left(\frac{\epsilon_x - \epsilon_y}{2}\right)^2 + \left(\frac{\gamma_{xy}}{2}\right)^2} \quad (3)$$

where  $\epsilon_{1,2}$  are principal strains, and  $\epsilon_x$ ,  $\epsilon_y$ , and  $\gamma_{xy}$  are normal and shear strains in the xy-plane.

The results for RR correlations with  $\epsilon_{HP}$  for AC, CI, and PVC pipelines are presented in Figures 5a through 5c. The screening criteria were applied using confidence levels of 95%, 85%, and 75% for AC, CI, and PVC pipelines, respectively. Comparison between RR correlations derived from 4-m and 56-m spacings of lateral strain shows significant differences for AC and PVC pipelines, whereas RR correlations for CI pipelines in Figure 5b derived from lateral strains at

56-m and 4-m spacing are within the same range.

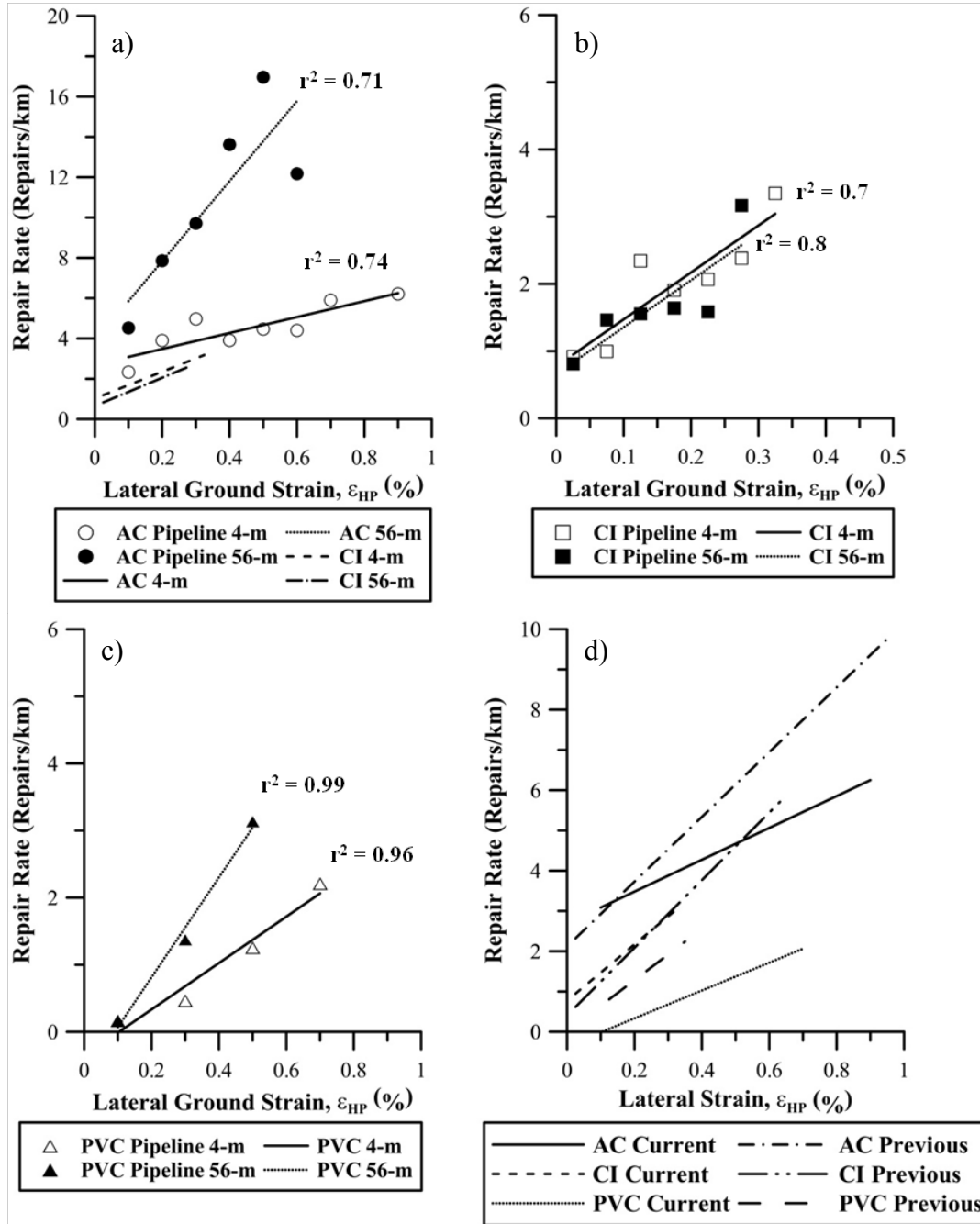


Figure 5. Correlations of repair rate with lateral ground strain at 4-m and 56-m spacing for a) AC, b) CI, and c) PVC pipe materials for the 22 Feb. 2011 earthquake, and d) comparison.

Lateral movements at 56-m spacing result in a relatively coarse lattice of lateral ground strains that does not capture the effects of locally high horizontal strain. The AC and PVC pipelines were concentrated in the eastern areas of Christchurch where locally high strain fields developed in response to liquefaction. In contrast, the CI pipelines were located in areas with significantly



more uniform strains than AC and PVC pipelines, resulting in reduced effects of grid size on the resulting RR vs  $\epsilon_{HP}$  correlations.

### Combined Effects of Differential Vertical Ground Movement and Lateral Ground Strain

The combined effects of lateral strain and differential vertical movement on pipeline damage were evaluated with an approach similar to that developed by Boscardin and Cording (1989) for ground movement effects on buildings. Pipeline RRs were correlated with both  $\beta$  and  $\epsilon_{HP}$  calculated from vertical and horizontal LiDAR movements at 5-m and 4-m spacing, respectively. The confidence level when screening the data was adjusted to 75% and 60% for AC and CI pipelines, respectively, to attain a broad distribution of data within the  $\beta$  vs  $\epsilon_{HP}$  space. Correlations among RR,  $\beta$ , and  $\epsilon_{HP}$  for AC and CI pipelines were developed, using the global polynomial interpolation method in ArcMap 10.1 (2012) with a first-order polynomial model. Both the data points that passed the screening criteria and the RR contours for AC and CI pipelines are shown in Figures 6a and 6b, respectively.

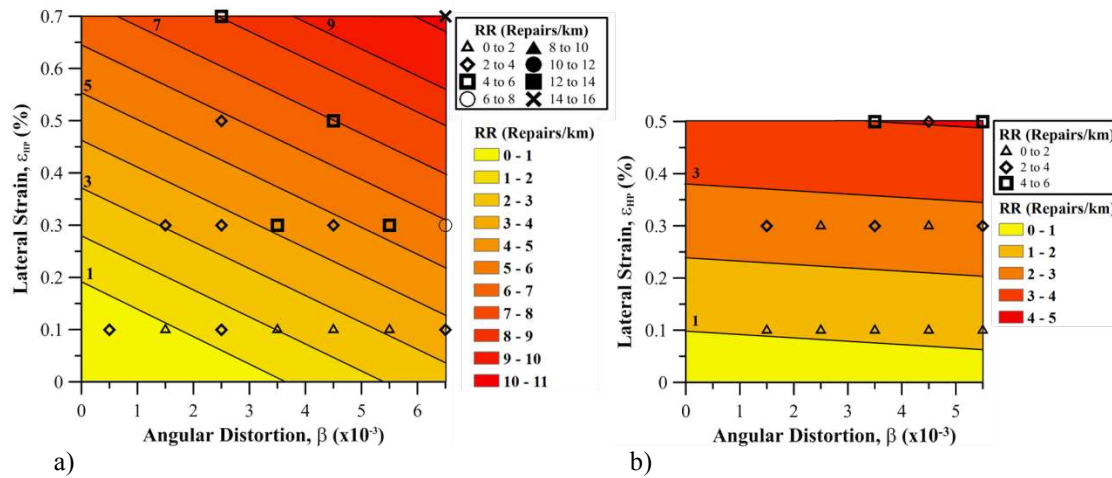


Figure 6. Repair rate vs. lateral ground strain and ground angular distortion for a) AC and b) CI pipelines.

The range of  $\beta$  vs  $\epsilon_{HP}$  covered by CI pipeline RRs is smaller than the range covered by AC pipelines. As shown in Table 1, there is a large number of AC pipeline repairs compared to CI pipeline repairs, and thus a more extensive database for AC repair sampling for combined  $\epsilon_{HP}$  and  $\beta$  effects.



## Conclusions

This paper expands on previous work by O'Rourke, et al. (2014). It uses more recent water pipeline repair data and thus benefits from additional raw data validation and screening. This study compares RR correlations with lateral strains developed on the basis of 4-m and 56-m spacing of LiDAR data, and thus provides insight with respect to the effects of scale on data reduction and associated regressions of pipeline repair data. The correlations among RR,  $\epsilon_{HP}$ , and  $\beta$  for AC and CI pipelines in this work are based on a more rigorous statistical screening and analysis of the data, and are a significant improvement over previous RR,  $\epsilon_{HP}$ , and  $\beta$  correlations.

The principal findings of this paper are:

- The Christchurch data for RR vs GMPGV provide for more robust regressions for future fragility analyses of water distribution pipeline performance during earthquakes which compare favorably with previous studies (O'Rourke et al., 2014).
- Repair regressions quantify the relative performance of different types of pipelines under different levels of  $\epsilon_{HP}$ , and  $\beta$ , and indicate that the segmented pipelines most resilient to PGD and TGD effects are PVC pipelines relative to AC and CI pipelines.
- Scale effects have a substantial impact on the inferred relationship between pipeline damage and lateral ground strain, and depend on local variations in the strain field. High resolution data are needed to capture the influence of localized ground deformation. Computational models that utilize such regressions need to account for scale effects.
- The correlations among RR,  $\epsilon_{HP}$ , and  $\beta$  for AC and CI pipelines in this work provide for the first time the means to predict RR on the basis of the combined effects of  $\epsilon_{HP}$ , and  $\beta$ . These correlations may be used in future planning, design, and loss estimation to assess limiting deformations for pipelines subjected to both PGD-induced lateral and vertical differential displacements.

## Acknowledgments

The work described in this paper was supported by the National Science Foundation (NSF) under Award No. 1137977 and the U.S. Geological Survey (USGS) under Grant No. G12AP20034.

## References

- ArcMap 10.1. Environmental Systems Resource Institute (ESRI): Redlands, California, 2012.
- Bouziou D. *Earthquake-induced ground deformation effects on buried pipelines*. PhD Thesis. Cornell University: Ithaca, New York, 2015.
- Boscardin MD, Cording, EJ. *Building response to excavation-induced settlement*. *Journal of Geotechnical Engineering* 1989; **115**(1):1-21.
- Canterbury Earthquake Recovery Authority (CERA). Geotechnical database for Canterbury Earthquake Sequence, NZ, available at: <https://canterburygeotechnicaldatabase.projectorbit.com>. [accessed June 2012]
- Geonet. Processed strong ground motions. Available at: <ftp://ftp.geonet.org.nz/strong/processed/Proc/2011/>. [accessed June 2013]
- Jeon S-S. *Earthquake performance of pipelines and residential buildings and rehabilitation with cast-in-place pipe lining systems*. Ph.D. Dissertation: Cornell University, Ithaca, NY, 2002.
- Jeon S-S, O'Rourke TD. *Northridge earthquake effects on pipelines and residential buildings*. *Bulletin of the Seismological Society of America* 2005; **95**(1): 294-318.

*O'Rourke TD, Jeon S-S, Toprak S, Cubrinovski M, Hughes M, van Ballegooy M, Bouziou D. Earthquake response of underground pipeline networks in Christchurch, NZ. Earthquake Spectra 2014; 30(1):183-204.*